The Feasibility of a Cochlear Nucleus Auditory Prosthesis Based on Microstimulation

Contract No. NO1-DC-5-2105
QUARTERLY PROGRESS REPORT #9
july 1,1997 - Sept 30,1997

HUNTINGTON MEDICAL RESEARCH INSTITUTES
Neurological Research Laboratory
734 Fairmount Ave
Pasadena, CA 91105

HOUSE EAR INSTITUTE
Departments of Auditory Implant Research and Neuroanatomy
2100 W. Third St.
Los Angeles, CA 90057

We are submitting the enclosed manuscript, "Accessing the tonotopic gradient of the ventral cochlear nucleus by intranuclear microstimulation" as our quarter progress report #9. The manuscript has been submitted to the IEEE Transaction on Rehabilitation Engineering.

Accessing the tonotopic organization of the ventral cochlear nucleus by intranuclear microstimulation

D.B. McCreery, Ph.D. (1)
R.V. Shannon, Ph.D. (2)
J.K. Moore Ph.D. (2)
Monita Chategee (2)

(1) **HUNTINGTON MEDICAL RESEARCH INSTITUTES**
NEUROLOGICAL RESEARCH LABORATORY
734 Fairmount Avenue
Pasadena, California 91105

---

(2) **HOUSE EAR INSTITUTE**
2100 WEST THIRD STREET
Los Angeles, California 90057

Address correspondences to:
Douglas McCreery, Ph.D.
Huntington Medical Research Institutes
Neurological Research Laboratory
734 Fairmount Ave., Pasadena, CA 91105

Running title: Microstimulation in the cochlear nucleus

ABSTRACT

This study is part of a program to develop an auditory prosthesis for the profoundly deaf, based on multichannel microstimulation in the cochlear nucleus. The functionality of such a device is dependent on its ability to access the tonotopic organization of the human ventral cochlear nucleus in an orderly fashion. In these studies we utilized the homologies between the human and feline ventral cochlear nuclei and the known tonotopic organization of the central nucleus of the inferior colliculus (IC). In anesthetized cats, stimuli were delivered to 3 or 4 locations along the dorsal-to-ventral axis of the posteroventral cochlear nucleus (PVCN) , and for each stimulus location, we recorded the multiunit neuronal activity and the field potentials at 20 or more locations along the dorsolateral-ventromedial (tonotopic) axis of the IC. The current source-sink density (CSD), which localizes regions of neuronal activity, was computed from the sequence of field potentials recorded along this axis. The multiunit activity and the CSD analysis both showed that the tonotopic organization of the PVCN can be accessed in an orderly manner by intranuclear microstimulation in several regions of the PVCN, using the range of stimulus pulse amplitudes that have been shown in previous studies to be non-injurious during prolonged intranuclear microstimulation via chronically implanted microelectrodes. We discuss the applicability of these findings to the design of a clinical auditory prostheses for implantation into the human cochlear nucleus.

INTRODUCTION

The auditory brainstem implant (ABI) can restore useful hearing to patients in whom both auditory nerves have been destroyed by tumors of the VIIIth cranial nerve (vestibular schwannomas), and who therefore cannot benefit from cochlear implants (1,2,3,4,5,6). The present version of the ABI consists of 8 platinum-Iridium disk electrodes on a silicone elastomer substrate. Following removal of the vestibular schwannoma, the electrode assembly is placed inside the lateral recess of the IVth ventricle, which positions the electrode adjacent to the cochlear nucleus. Most ABI patients report different pitch sensations when different electrodes are pulsed, suggesting that these surface electrodes have some limited ability to access the tonotopic dimension of the human cochlear nucleus. However, the overall performance level of patients with the surface-electrode ABI is considerably poorer than average performance of patients with a multi-channel cochlear implant (7,8,9). One possible reason for this difference is the relatively poor access to the tonotopic axis of the cochlear nucleus, as compared to the cochlear implant. Indeed, the few ABI patients who show the highest level of speech recognition also have the widest range of pitch sensations across the 8 surface electrodes. Unfortunately, direct access to the tonotopic gradient of the human cochlear nucleus is limited with surface electrodes. An array of electrodes on the surface of the brainstem can activate neurons throughout most of the underlying cochlear nucleus, but can provide only limited access to the ordered mapping of acoustic frequencies (the tonotopic gradient) within the ventral cochlear nucleus, whereas an array of microelectrodes that penetrates down into the nucleus could, at least in principle, allow more precise and orderly access to the gradient. Thus, a prosthesis employing both type of electrodes might provide the patients with improved hearing.

The posteroventral cochlear nucleus (PVCN) and the posterior position of the anteroventral cochlear nucleus (AVCN) are the preferred locations for an intranuclear auditory prosthesis, since the multipolar (stellate) neurons of this region project to the

nuclei of the lateral lemniscus and to the inferior colliculus, and therefore, appear to be the cell population that mediates monaural hearing (10,11,12). A cochleotopic (tonotopic) sequence of auditory nerve axons has been demonstrated in cat by studies involving axonal degeneration (13,14,15,16) and axonal transport (17,18). Electrophysiological recordings (19,20) have confirmed that high frequencies are represented in the dorsalmost axons, with a continuous gradient down to the low frequencies in the ventral axons. However, in addition to exciting the neuronal cell bodies, intranuclear microstimulation might excite the axons (both afferent and efferent) or the dendrites of neurons that branch and traverse within the neuropil of the PVCN and this could make it difficult to access the tonotopic organization of the ventral nucleus by intranuclear microstimulation. Nevertheless, the basic feasibility of accessing the tonotopic organization of the ventral cochlear nucleus by intranuclear microstimulation has been establish in the cochlear nucleus of the guinea pig, using multi-site silicon substrate microprobes (21). The present study was conducted to determine the feasibility of accessing the tonotopic gradient of the PVCN by intranuclear microstimulation, using the range of stimulus current amplitudes shown to be safe and effective in previous studies with prolonged stimulations using chronically-implanted microelectrodes in adult cats (22,23,24), a species in which the spatial dimension and internal organization of the ventral cochlear nucleus are similar to the human.

METHODS

Adult cats of either sex were anesthetized with Halothane and nitrous oxide. Part of the cerebellum was aspirated to expose the cochlear nucleus, and part of the occipital pole of the cerebrum was resected to expose the contralateral inferior colliculus. The iridium recording and stimulating microelectrodes had exposed geometric surface areas of approximately 500 μm^2. In each animal, the stimulating microelectrode was positioned at each of 3 or 4 locations along the dorsal- to- ventral tonotopic gradient of the posteroventral cochlear nucleus. The stimulus delivered in

the PVCN was a single controlled-current, charge balanced triphasic pulse, 8 to 24 μA in amplitude, at 25 Hz. The duration of the cathodic phase was 150 μsec, and the first and third (anodic) phases also totaled 150 μsec, and were partitioned to minimize the stimulus artifact. While stimulating at each location in the PVCN, the evoked potential and multiunit activity were recorded along the dorsolateral--ventromedial (DLVM) axis of the contralateral inferior colliculus. This axis is approximately along the tonotopic gradient of the colliculus (25,26,27,28). The recording electrode was advanced through the colliculus at an angle of 45° above the horizontal plane. At intervals of 100 or 200 μm along this track, the gross evoked potential was averaged, and multiunit activity was recorded during 512 consecutive presentations of the electrical stimulus in the PVCN. To record the activity of the individual neurons in the inferior colliculus, the signal from the recording amplifier was sent through a 6-pole band pass filter (2-10 KHz). For the gross evoked potential, a 2-pole filter with a band pass of 20 Hz to 2.5 KHz was used.

The action potentials from several neural units in the IC (multi-unit activity, MUA) was recorded simultaneously with the aid of SOLO, a custom software package. This software detects as an event, any signal level that exceeds a certain threshold which is determined automatically by analysis of the background noise and spontaneous neural activity in the absence of any electrical stimulation. The criterion was set so that there would be an average of 2 spontaneous events during each recording interval (following each stimulus pulse).

Current source density (CSD) has also proven to be useful as a means of localizing neural activity. The technique locates regions within the tissue volume in which current is passing from the extracellular compartment into (or out of) a spatially extensive intracellular compartment. The latter might be myelinated axons or the apical dendrites of large neurons. The CSD at point x,y,z within the tissue volume represents the net current flowing in or out of the neural elements and is given by:

$$I_{d(x,y,z),} = -[\, \sigma_x \, \delta^2 \phi/\delta x^2 + \sigma_y \, \delta^2 \phi/\delta y^2 + \sigma_z \, \delta^2 \phi/\delta y^2 \,] \qquad (1)$$

where ϕ is the field potential at x,y,z, and σ_x, σ_y and σ_z are the principal tissue conductances (29). To compute equation 1, the extracellular field potential must be measured simultaneously at 7(or more) points, at and around x,y,z. However, in situations in which the neuronal responses to the stimulation are quite constant over time and in which the tissue is nearly isotropic ($\sigma x \cong \sigma y \cong \sigma z \cong \sigma$) , as has shown to be the case in the central nucleus of the inferior colliculus (26), then the current source density can be computed from measurements of the averaged evoked potential obtained along a single axis (26,27).

Freeman and Nicholson (29) described and compared various smoothing procedures for reducing the noise inherent in the calculation of the 2nd spatial derivative of ϕ, while maintaining the essential spatial resolution. We found that for our data, their 5-point formula gives the best trade-off between low noise and spatial resolution:

$$I_{d(x,y,z),} \cong D(x,y,z)= (0.01\ \sigma/h^2)[-2\phi(x-2h) - \phi(x-h) - 2\phi(x) + \phi(x+h) + 2(x+2h)] \qquad (2)$$

where h is the spacing between the points at which ϕ is measured. This formula is computationally equivalent to obtaining a least-squares error fit of a cubic polynomial to 5 successive data points along the axis of measurement, and then computing the second derivative of the fitted polynomial.

The two methods (MUA and CSD analyses) are complementary as means of localizing stimulation-induced neural activity. MUA analysis can best reveal the details of the neural activity at low stimulus amplitudes, near response threshold, where the CSD is vulnerable to the poor signal-to-noise ratio of the field potential. Conversely, the CSD analysis best quantifies the totality of the neural response at higher stimulus amplitudes, since it is not subject to some of the problems of quantitation that afflict MUA analysis (e.g, deciding whether a large spike originates from neuron that is large or close to the recording microelectrode, as opposed to several small or more distant neurons firing in close temporal synchrony)

At the end of the experiment, the stimulating and recording microelectrodes were fixed in place by flooding the craniectomies with melted dental wax. The cats were then deeply anesthetized with Nembutal and perfused through the heart with fixative (½ strength Karnovsky's solution) so that the location of the recording and stimulating electrodes could be identified in histologic sections.

RESULTS

Data were obtained from 5 cats. Figure 1A shows a histologic section through the right posteroventral cochlear nucleus (PVCN) of cat A4. This section is approximately in the frontal plane , but is slightly oblique to the track of the stimulating microelectrode. The dashed line is a reconstruction of the stimulating microelectrode's track through the nucleus and estimates of the locations of the four stimulating sites are based on reconstruction of the track from adjacent sections and on the location of the tip of the microelectrode when fixed in situ. Figure 1B is a photomicrograph of the PVCN adjacent to the microelectrode track. It shows a number of multipolar (stellate) neurons which are known to project via the trapezoid body to the nuclei of the lateral lemniscus and to the contralateral inferior colliculus.

Figure 2 shows the averaged evoked potential recorded in the contralateral inferior colliculus (IC) of cat CNA4 while stimulating in the PVCN. The response was evoked by stimulating with pulses 16 μA in amplitude, delivered at location #1 in Figure 1. The lower trace shows the multiunit activity recorded after a single stimulus pulse, at the same location in the IC. Figures 3A and 3B are contour plots of the multiunit activity recorded in the IC, for two pulse amplitudes (8 or 24 μA) and while stimulating at two locations in the contralateral PVCN. The ordinate is the time latency after each stimulus pulse in the PVCN, and the abscissa is the depth below the dorsolateral surface of the IC, along the dorsolateral-ventromedial (DLVM) axis. The plots illustrate that when the stimulus amplitude is low (8 μA), the neural activity is more localized, both in time after the stimulus and in depth in the inferior colliculus.

Figure 4 shows plots of the average number of events (spikes) elicited by each 16 μA stimulus pulse at 4 different stimulation sites along the dorsoventral axis of the PVCN, and plotted against depth in the contralateral inferior colliculus. As the site of stimulation was moved dorsally in the PVCN, the place of maximum response moved dorsally in the IC. It is notable that the magnitude of the maximum response did vary somewhat for different stimulation sites in the PVCN. Figure 5 shows another representation of the data from the same animal. The site of stimulation in the PVCN is plotted against the depth of the maximum response in the IC, for stimulus pulse amplitudes of 8, 16 and 24 μA. (1.2, 2.4 and 3.2 nC/phase). The plots demonstrate that the microstimulation is accessing the tonotopic organization of the PVCN.

Figure 6A shows stacked plots of the averaged evoked potential recorded at increments of 200 μm along the DLVM axis of the IC in the same animal, while stimulating with 24 μA at point 1 in the PVCN (Figure 1A) . The potential was largest at a depth of 2,000 μm below the surface of the I.C. along the DLVM axis, but the depth at which the potential is largest is rather poorly defined. Figure 6B shows the current source-sink densities computed from these evoked potentials. The maximum of the current sink (negativity) also is centered 2,000 μm below the dorsolateral surface of the colliculus, and is quite well localized along the DLVM axis. The negativity represents current flowing from the extracellular compartment and corresponds to active depolarization of neural elements. There is a current source below 2,400 μm that occurs simultaneously with the more superficial current sink, and this may represent the passive outflow of current from the axons of these neurons prior to initiation of active action potentials.

Figure 7A shows the amplitude of the negative phase (current sink) of the CSD signals that are plotted in Figure 6. The negativity is plotted against depth along the DLVM axis of the IC, for each of the 4 stimulating sites in the PVCN. The stimulus pulse amplitude was 24 μA. The peaks are fairly well separated for stimulation sites 500 μm apart dorsoventrally in the PVCN. The location of the peaks is in good agreement with the multi-unit response data (Figure 4). The multi-unit analysis and

the CSD analysis both show that different amounts of neural activity are evoked by stimulus pulses of the same amplitude when the stimulus is applied at different points along the dorsoventral axis of the PVCN. However, as we noted in Methods, the CSD analysis probably is a more reliable means of quantifying the amount of neuronal activity induce by a stimulus.

In the animal described above (CNA4), the stimulating microelectrode passed through the center of the PVCN (Figure 1A). Figure 7B shows the current sink data from another cat, in which the track of the stimulating microelectrode was close to the medial margin of the PVCN, near the place where the efferent axons converge before entering the trapezoid body (9). In this animal, there is less separation than in Figure 5A, of the neural activity in the IC for different stimulation sites in the PVCN, but the activity spans a wider range of depths in the IC (i.e., acoustic frequencies). This is in keeping with the findings of Snyder et al (14) that the full range of acoustic frequencies are represented only in the medial part of the PVCN. Figure 7C shows data from a third animal, in which the track of the stimulating microelectrode was more rostral in the PVCN, just caudal to the nerve root . (By convention, the root of the auditory nerve is taken as the demarcation between the anteroventral and posteroventral nuclei). Again, the separation of neural activity along the tonotopic gradient of the central nucleus of the IC was quite good for a stimulus amplitude of 20 μA, when the stimulation sites were separated by 500 μm.

DISCUSSION

Through the use of multiunit recording and current density analysis in the central nucleus of the inferior colliculus, we have demonstrated that intranuclear microstimulation allows an orderly access to the tonotopic organization of the posteroventral cochlear nucleus in the cat. In these acute mapping studies, we used iridium microelectrodes that are similar to those implanted chronically in the cat's posteroventral cochlear nucleus (22,23,24). The range of stimulus pulse amplitudes used in this study (8 to 24 μA, 1.2 to 3.6 nCoulombs/phase) spans the range that would be appropriate for prolonged microstimulation in the posteroventral cochlear nucleus of a human. In animal studies, we have found that if the stimulus amplitude exceeds 3 nC/phase (20 μA with a phase duration of 150 μsec), then tissue injury (23) and/or marked depression of neuronal excitability (24) may occur. As illustrated in Figure 3, the tonotopic organization of the PVCN can be accessed more selectively when the current pulse amplitude is low, presumably due to the limited spread of current from the stimulating microelectrodes. However, our data indicate that over the range of 8-24 μA, it should be possible to convey at least 4 separate channels of acoustic information into the cochlear nucleus using microelectrodes spaced 300-500 μm apart along the dorsoventral axis. In human subjects, 4 channels appears to be sufficient for good intelligibility of speech (31).

Both the multiunit analysis (Figure 3) and the current density analysis (Figure 7) show that stimulation at identical amplitudes evokes different amounts of neural activity in the inferior colliculus when applied at different depths in the PVCN. In the three cats described here, the largest response was recorded approximately 2 mm below the dorsolateral surface of the colliculus, and this corresponds to an acoustic frequency of approximately 4 kHz (22). We are uncertain as to the neuroanatomical organization underlying this variability, but in a clinical prosthesis based on intranuclear stimulation, it may be necessary to scale the amplitude of the stimulus delivered to each microelectrode, according to their location along the tonotopic gradient of the ventral

cochlear nucleus.

In order to apply the data obtained from the cat to the design of an auditory prosthesis for clinical use in humans, we must consider the similarities and differences of the feline and human ventral cochlear nuclei. As noted in the Introduction, a cochleotopic (tonotopic) sequence of auditory nerve axons has been demonstrated in cats' cochlear nucleus, in which there is a continuous gradient from low to high acoustic frequencies along the dorsoventral axis of the nucleus. Judging from myelin-stained sections of the human brain stem, the axonal organization of the human ventral nucleus is very similar to that of the cat (Figure 8A and 8B). Afferent fibers of the auditory nerve bifurcate within the nerve root to form an orderly sequence of axon fascicles crossing the anteroventral and posteroventral divisions of the nucleus. When compared to the cat, the dorsoventral elongation of the human nucleus appears to make the axonal planes more oblique, but the organization of the ascending and descending auditory nerve branches is so similar to that of other mammals that we assume a similar tonotopic organization. Though the auditory nerve itself is destroyed during resection of a tumor of the VIIIth nerve, and its fibers will degenerate within a few days after surgery, the neurons in the PVCN survive (32) and the tonotopic organization of the nucleus presumably persists. It is also important to consider the trajectory of the efferent axons of ventral nucleus relay neurons. In the cat, efferent axons traverse medially and slightly ventrally across the nucleus, parallel to its isofrequency laminae. The same appears to be true in the human ventral nucleus (33). Thus, in both species, they course nearly parallel to the isofrequency lamina of the ventral nuclei. Were this not the case, the stimulating microelectrodes might excite axons from many different isofrequency laminae, and this could make it much more difficult to access the nucleus's tonotopic organization in an orderly manner.

Analyses of the cytoarchitecture of the human cochlear nuclei (33,34) reveal that the same cell types are encountered as in the cat, though in somewhat different proportions. In both species, the ventral nucleus consists of a rostral area of spherical cells, a caudal area of octopus cells, and an intervening central region where globular

cells, multipolar cells and small cells are intermingled. However, the size of the spherical and octopus cell populations appears to be reduced in the human ventral nucleus, probably due to changes in their target nuclei in the superior olivary complex (33). In man, there is also a relatively large cap area which lies outside the field of the primary fibers, covering the lateral surface of the ventral nucleus and rising high above it dorsally (Figure 8). Thus within the ventral nucleus, we assume that the optimal region for microstimulation would be the central area (mostly co-incident with the PVCN in Figure 8) , where the multipolar neurons projecting directly to the inferior colliculus are concentrated. Since the microelectrode array would be inserted from the ventral brainstem surface, the electrodes would lie orthogonal to the tonotopic gradient, and different parts of the gradient could be accessed by electrodes of different lengths.

Figure 9 illustrates the similarity between the human and feline cochlear nucleus complex. The human ventral cochlear nucleus seems to be slightly smaller than that of the cat, with a span of about 3 mm in all dimensions. The central area presumably includes a full representation of the tonotopic gradient. We thus believe that the human and cat ventral nuclei are sufficiently similar to allow the cat to serve as a model for electrode design and testing.

FIGURES:

Figure 1 (A) A histologic section, slightly oblique to the frontal plane, through the right posteroventral cochlear nucleus (PVCN) of cat A4 The overlay is a reconstruction of the stimulating microelectrode's track through the nucleus. Estimates of the locations of the four stimulating sites are labeled 1,2,3,4 (Bar = 300 μm)..
(B) A photomicrograph of the PVCN adjacent to the microelectrode track, showing a number of multipolar (stellate) neurons (Bar = 50 μm).

Figure 2. An averaged evoked potential (n = 512) recorded in the inferior colliculus of cat A4 while stimulating in the PVCN. The response was evoked by stimulating with pulses 16 μA in amplitude, delivered at location #1 in Figure 1. The lower trace shows the corresponding multiunit activity evoked by one stimulus pulse. Both traces were recorded at the same location in the inferior colliculus.

Figure 3. Contour plots of the multiunit activity recorded in the inferior colliculus while stimulating at two pulse amplitudes (8 or 24 μA) and at two locations in the contralateral PVCN. The ordinate is the time latency after each stimulus pulse in the PVCN, and the abscissa is the depth below the dorsolateral surface of the inferior colliculus, along the dorsolateral-ventromedial (DLVM) axis. The numbers beside the contour lines indicate the total number of spikes collected in each 50 μsec bin, during 512 consecutive presentations of the stimulus pulse.

Figure 4 A plot of the average number of events (neurons units) evoked after each presentation of the stimulus pulse at different sites in the PVCN, and plotted against depth in the contralateral inferior colliculus. The stimulation sites are with respect to the labeled sites along the electrode track shown in Figure 1. 512 responses were averaged to obtain each response.

Figure 5 A plot of the depth of the maximum response evoked in the inferior colliculus a range of stimulus amplitudes delivered at different stimulation sites in the PVCN.

Figure 6. (A) Stacked plots of the averaged evoked potential recorded at increments of 200 μm along the dorsolateral-medioventral (DVLM) axis of the inferior colliculus in cat CNA4. The responses were obtained while stimulating with 24 μA at point 1 in the PVCN (Figure 1A) . (B) The current source-sink densities computed from these evoked potentials, according to Equation 2 of Methods.

Figure 7. (A) Plots of the amplitude of the negative phase (current sink) of the CSD signal that is shown in Figure 4. The negativity is plotted against depth in the inferior colliculus, for each of the 4 stimulating sites in the PVCN, numbered 1,2,3,4 in Figure 1A. The stimulus pulse amplitude was 24 μA. (Figure 4B,C): Similar plots of the current sink from two additional cats, in which the stimulating microelectrodes was in different parts of the posteroventral cochlear nucleus. The plots have been smoothed using a cubic spline interpolation.

Figure 8. A diagrammatic representation of the human and feline cochlear nucleus complexes, seen in lateral views. The portion of the central nucleus containing the stellate/multipolar cells is stippled (Reprinted from Moore and Olsen ,1979, by permission of the publisher).

Figure 9. A section through the human ventral cochlear nucleus. The material has been embedded in celloidin and sectioned along the long axis of the nucleus in a rotated sagittal plane (anterior end rotated outward 30°, as shown in the insert drawing of the brainstem as seem from its dorsal surface). The section has been stained with Cresyl violet and iron hematoxylin to demonstrate both cells and myelinated nerve..

The superficial posterior surface of the nucleus is covered by the pontobulbar body (PBB). Individual fibers of the auditory nerve bifurcate within the nerve root (ANR). The direction of the diverging terminal branches within the anteroventral and posteroventral divisions of the nucleus (AVCN, PVCN) is indicated by arrows. Areas of spherical cells (sph), octopus cells (oct), and the small cell cap (cap) are indicated. (Bar= 500 μm)

Acknowledgments:

We thank Ms. Edna Smith for assistance with the animal surgeries, Ms. Anne Hite and Mr. Clarence Graham and Brian Wu for able technical assistance in the preparation of the histologic material and photographs, and Ms. Cheryl Long for secretarial assistance. We an indebted to Dr. Russell Snyder (Epstein Laboratory, University of Calif , San Francisco, Ca.) for his assistance in developing the animal preparation. The original version of the SOLO data acquisition program was written by Wes Wang.

This work was supported by Contracts No NO1-DC-2400 and NO1-DC-5-2105. from the National Institutes of Health (NIDCD). This work was conducted using a protocol approved by the HMRI Institutional Animal Care & Use Committee, and the study was conducted according to the committee's standards .

We thank Springer-Verlag Inc (New York), for permission to reprint Figure 9.

REFERENCES

1. L.S. Eisenberg, A.A., Maltan, F. , Portillo, J.P., Mobley,. and W.F. House, W.F. " Electrical stimulation of the auditory brain stem in deafened adults" J. Rehab. Res. Dev vol 24 pp:9-22, 1987

2. R. V. Shannon, "Threshold functions for electrical stimulation of the human cochlear nucleus," *Hear. Res.*, vol. 40, pp. 173-178, 1989.

3. R. V. Shannon and S. R. Otto, "Psychophysical measures from electrical stimulation of the human cochlear nucleus," *Hear. Res.*, vol. 47, pp. 159-168, 1990.

4. D.E. Brackmann, W.E. Hitselberger, R.A. Nelson, J.K. Moore, M. Waring, F. Portillo, R.V. Shannon, and F.Telischi " Auditory Brainstem Implant. I: Issues in Surgical Implantation" *Otolaryngology, Head and Neck Surgery, 108, 624-634, 1993.*

5. R. V. Shannon, J. Fayad, J. K. Moore, W. Lo, M. O'Leary, S. R. Otto, and R. A. Nelson, "Auditory brainstem implant. II: Post-surgical issues and performance," *Otolaryngol., Head Neck Surgery,* vol. 108, pp. 635-643, 1993.

6. S. A. Otto, R. V. Shannon, D. E. Brackmann, W. E. Hitselberger, S. Staller, and C. Menapace, "The multichannel auditory brainstem implant: Performance in 20 patients," *Otolaryngol., Head Neck Surgery,* in press, 1997.

7. Fishman K., Shannon R.V. and Slattery W.H. "Speech recognition as a function of the number of electrodes used in the SPEAK cochlear implant speech processor". *Journal of Speech and Hearing Research*, in press.

8. B.J. Gantz, R.S. Tyler, B.F. McCabe, J Preece, M.W. Lowder, and S.R. Otto " Iowa cochlear implant program: results with two single-channel and one multi-channel cochlear implants " *Laryngoscope vol 95, pp 443-449, 1985*

9. C.L. Parkins, D.K. Eddington, J.L. Orth, and D.E. Brackmann "Speech recognition with multichannel cochlear implants" *Otolarynolgol. Head & Neck Surg. vol 93: pp 639-645, 1985*

10. N.B. Cant "Identification of cell types in the anteroventral cochlear nucleus that project to the inferior colliculus," *Neurosci. Letters*, vol. 32, pp. 241-246, 1982.

11. J.K. Brunso-Bechtold., G.C. Thompson, and R.B.Masterton "HRP study of the organization of the auditory afferents ascending to central nucleus of the inferior colliculus in cat," *J. Comp. Neurol.*, vol. 197, pp. 705-722, 1981.

12. W.B. Warr " Fiber degeneration following lesions in the multipolar and globular cell areas in the ventral cochlear nucleus of the cat," *Brain Res.*, vol. 40, pp. 247-270, 1972.

13. T.P.S.Powell and W.M. Cowen " An experimental study of the projection of the cochlea," *J. Anat.*, vol. 96, pp. 269-284, 1962.

14. I. Sando, "The anatomical relationships of the cochlear nerve fibers," *Acta Oto-Laryngol.*, vol. 59, pp. 417-435, 1965.

15. K. K. Osen, "Course and termination of the primary afferents in the cochlear nuclei of the cat: An experimental anatomical study," *Arch. Ital. Biol.*, vol. 108, pp. 21-51, 1970

16. A.R. Arnesen and K.K. Osen "The cochlear nerve in the cat: Topography, tonotopy and fiber spectrum," *J. Comp. Neurol.*, vol. 147, pp. 281-290, 1978.

17. R. L. Snyder, P. A. Leake, and G. T. Hradek, "Quantitative analysis of spiral ganglion projections to the cat cochlear nucleus," *J. Comp. Neurol.*, vol. 379, pp. 133-149, 1997.

18. Fekete, D.M., Rouiller, E.M., Liberman, M.C. and Ryugo, D.K., "The central projections of intracellularly labeled auditory nerve fibers in cats," *J. Comp. Neurol.*, vol. 229, pp. 432-450, 1984.

19. J. E. Rose, R. Galambos, and J. Hughes, "Organization of frequency sensitive neurons in the cochlear nuclear complex of the cat," in *Neuronal Mechanisms of the Auditory and Vestibular Systems,* G. L. Rasmussen and W. F. Windle, Eds. Springfield: C. C. Thomas, pp. 116-136, 1960.

20. T. R. Bourke, J. M. Mielcarz, and B. E. Norris, "Tonotopic organization of the anteroventral cochlear nucleus of the cat. *Hear. Res.*, vol. 4, pp. 215-241, 1981.

21. D.A.Evans, J.K.Niparko, R.A. Altschuler, K.A. Frey, and J.A. Miller " Demonstration of prosthetic activation of central auditory pathways using [^{14}C]-2-Deoxyglucose" *Laryngoscope, 100, 128-13, 1990*

22. D.B McCreery, T.G.H. Yuen, W.F. Agnew and L.A. Bullara " Microstimulation in the cochlear nucleus of the cat with chronically implanted microelectrodes: Histologic and physiologic effects". *Hearing Res. vol 62 pp. 42-56, 1992*

23. D.B McCreery, T.G.H. Yuen, W.F. Agnew and L.A. Bullara " Stimulation parameters affecting tissue injury during microstimulation in the cochlear nucleus of the cat" *Hearing Research vol 77 pp.105-115, 1994 .*

24. D.B. McCreery, T.G.H. Yuen, W.F. Agnew, W.F. and L.A. Bullara, " A characterization of the effects on neuronal excitability resulting from prolonged microstimulation with chronically implanted microelectrodes". *IEEE Trans. Biomed. Eng. 44:931-939*

25. M. Brown, W. R. Webster, and R. L. Martin, "The three-dimensional frequency organization of the inferior colliculus of the cat: A 2-deoxyglucose study," *Hear. Res.,* vol. 104, pp. 57-72, 1997.

26. D. M. Harris, "Current source density analysis of frequency coding in the inferior colliculus," *Hear Res.,* vol. 25, pp. 257-266, 1987.

27. D.M. Harris, R.V. Shannon, R. Snyder. and E. Carney, E. " *Multi-unit mapping of acoustic stimuli in gerbil inferior colliculus"* Hearing Research, 108, 145-156,1997.

28. A. F. Ryan, J. M. Miller, Z. Wang, and N. K. Woolf, "Spatial distribution of neural activity evoked by electrical stimulation of the cochlea," *Hear. Res.,* vol. 50, pp. 57-70, 1990.

29. J. A. Freeman and C. Nicholson, "Experimental optimization of current source-density technique for anuran cerebellum,"*J. Neurophysiol.* vol.38, pp. 369-382., 1975

30. W.A. Hagins, R.D. Penn and S. Yoshikami, " Dark currents and photo currents in retina rods" *Biophysics J. vol 10 pp. 380-412 , 1970*

31. R. V. Shannon, F. Zeng, V. Kamath, J. Wygonski, and M. Ekelid, "Speech recognition with primarily temporal cues," *Science,* vol. 270, pp. 303-304, 1995.

32: Quarterly Progress Report #4, NIH contract N)1-DC-2400 " Feasibility of a central nervous system auditory prosthesis"

33. J. K. Moore and K. K. Osen, "The cochlear nuclei in man *" Amer. J. of Anat. vol. 154(3)pp. 393-417, 1979*

34. J. K. Moore, "The human auditory brain stem: A comparative view," *Hear. Res.,* vol. 29, pp. 1-32, 1987.

35. J.K. Moore, J.K. and R.Y. Moore "A comparative study of the superior olivary complex in the primate brain,",Folia Primat., vol. 16, pp. 35-51, 1971.

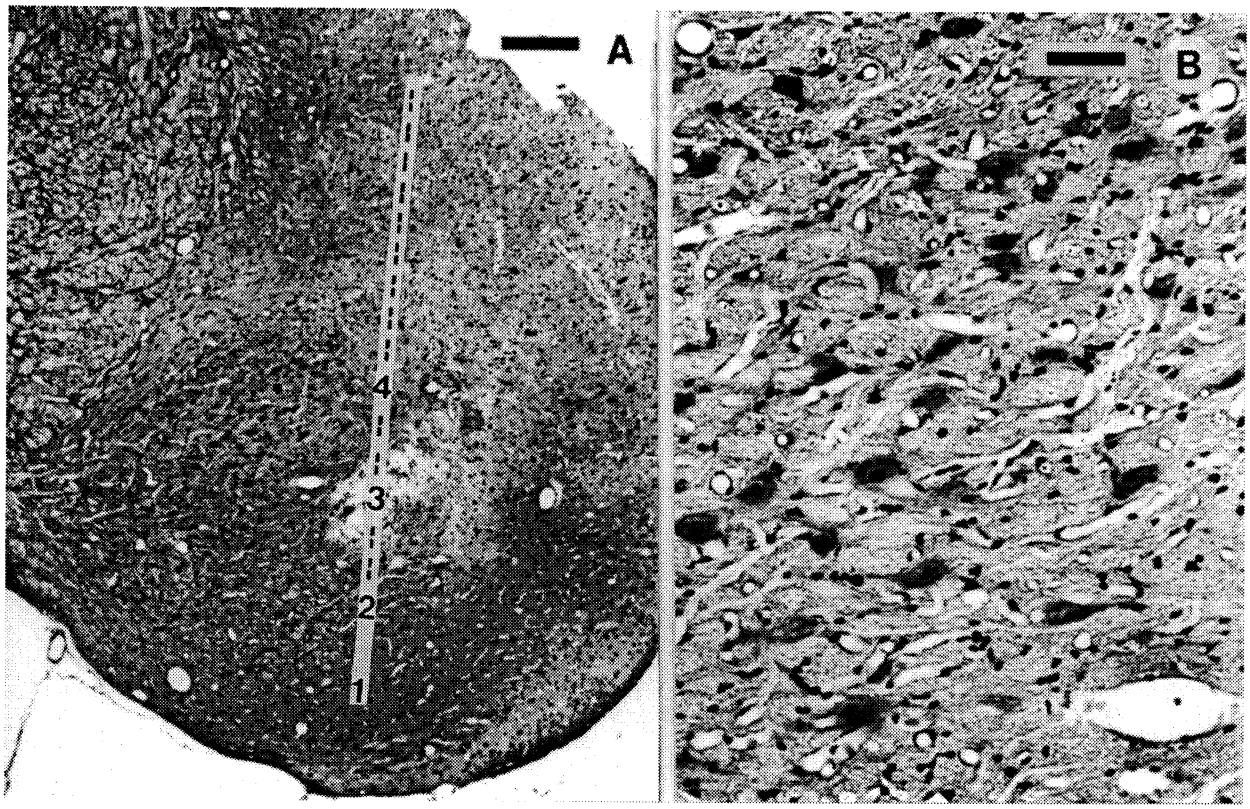

Figure 1

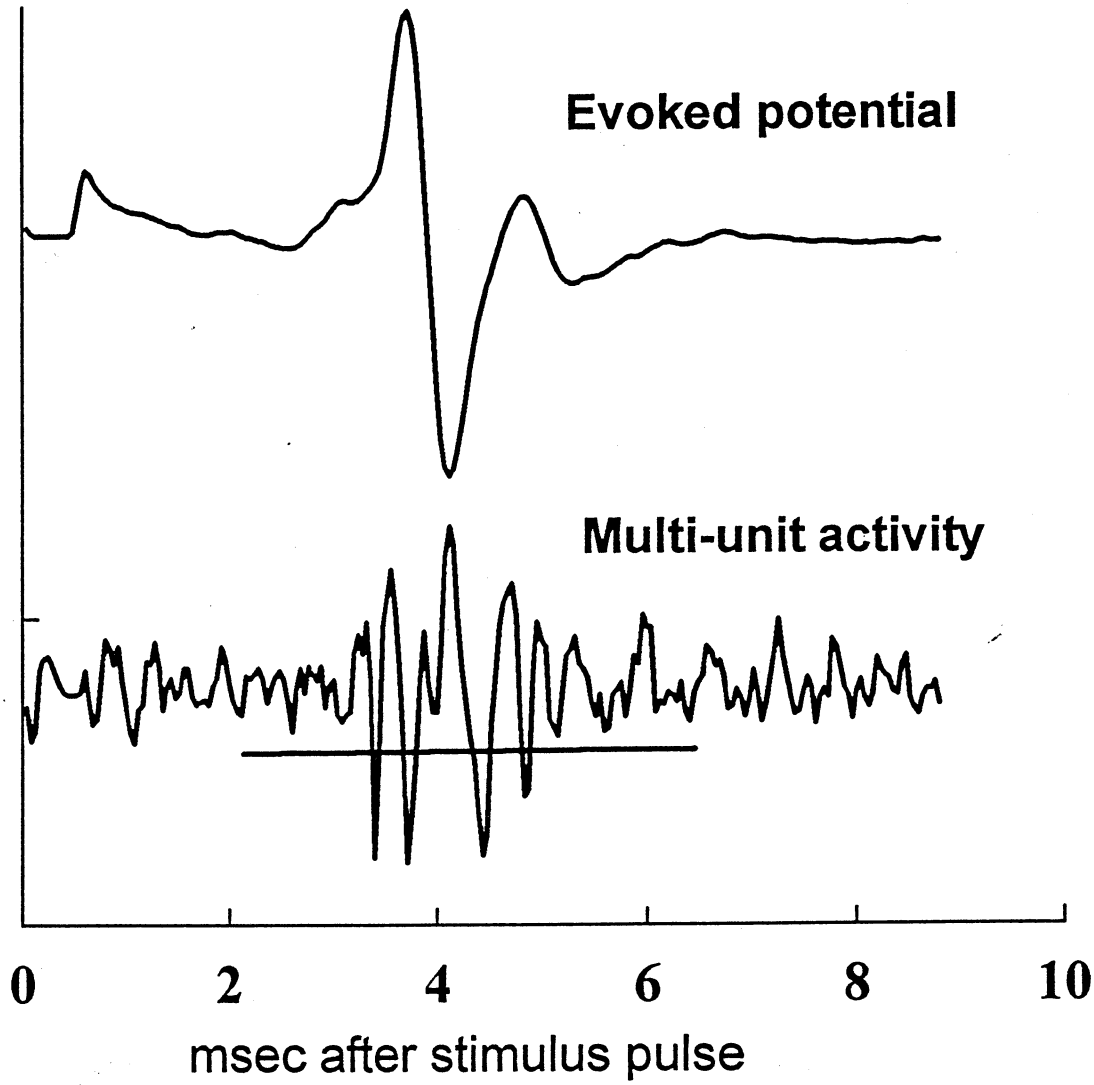
Evoked potential
Multi-unit activity
0
2
4
6
8
10
msec after stimulus pulse

Figure 2

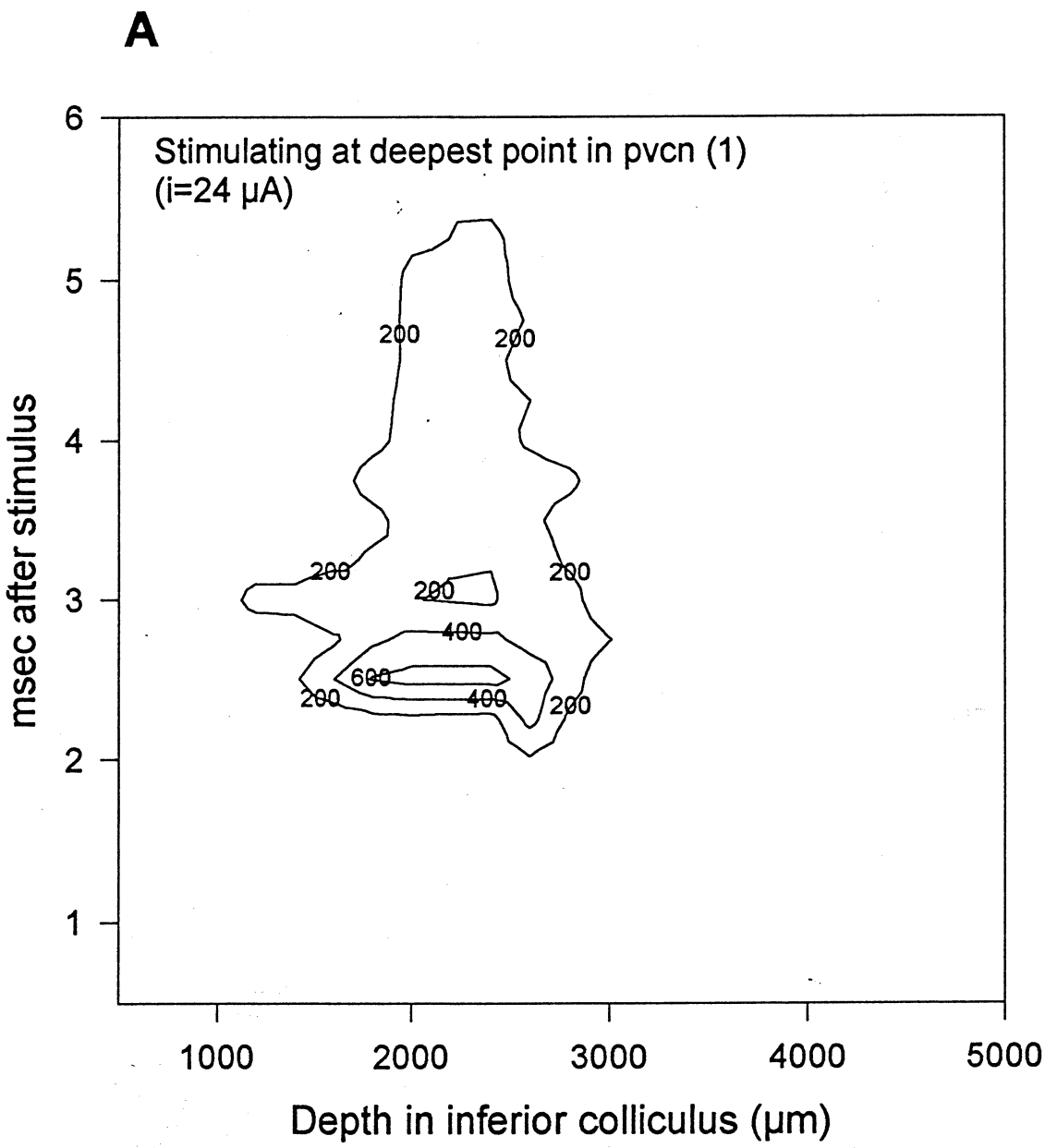
A
Stimulating at deepest point in pvcn (1)
(i=24 µA)
200
200
200
200
200
400
600
200
400
200
msec after stimulus
1
2
3
4
5
6
1000
2000
3000
4000
5000
Depth in inferior colliculus (µm)

Figure 3A

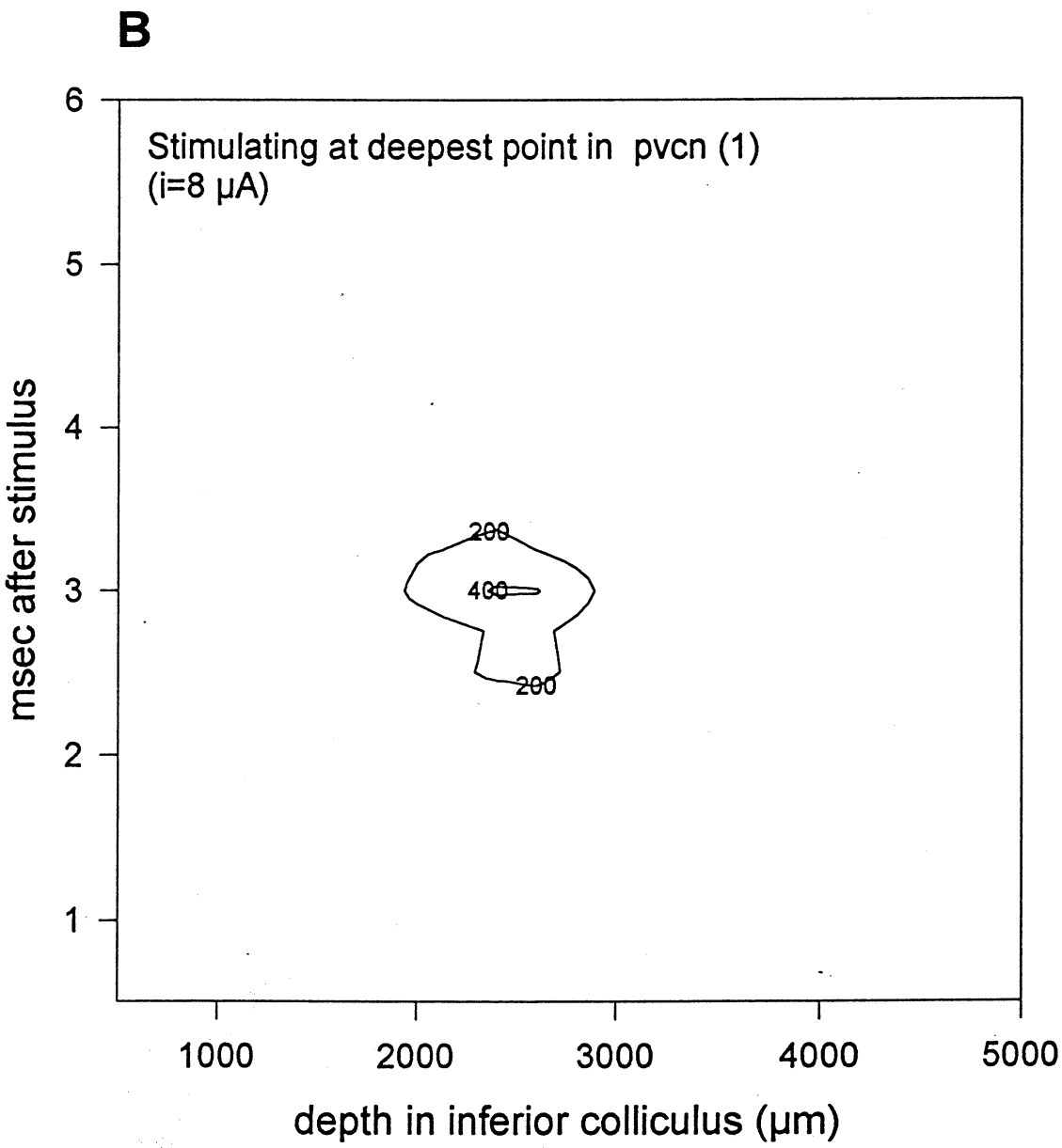
B
Stimulating at deepest point in pvcn (1)
(i=8 µA)
200
400
200
msec after stimulus
6
5
4
3
2
1
1000
2000
3000
4000
5000
depth in inferior colliculus (µm)

Figure 3B

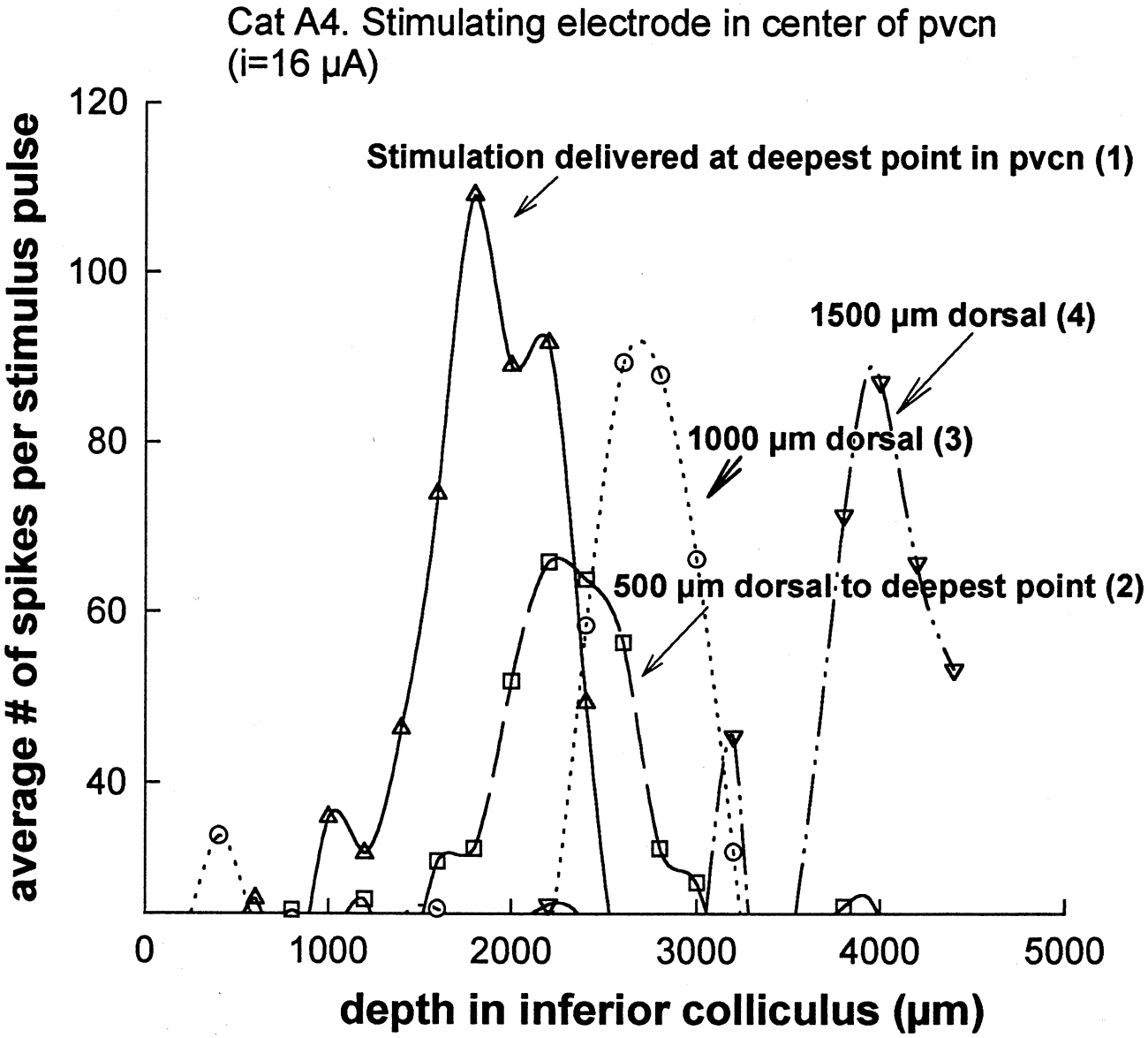
Cat A4. Stimulating electrode in center of pvcn
(i=16 µA)
Stimulation delivered at deepest point in pvcn (1)
1500 µm dorsal (4)
1000 µm dorsal (3)
500 µm dorsal to deepest point (2)
average # of spikes per stimulus pulse
depth in inferior colliculus (µm)
120
100
80
60
40
0
1000
2000
3000
4000
5000

Figure 4

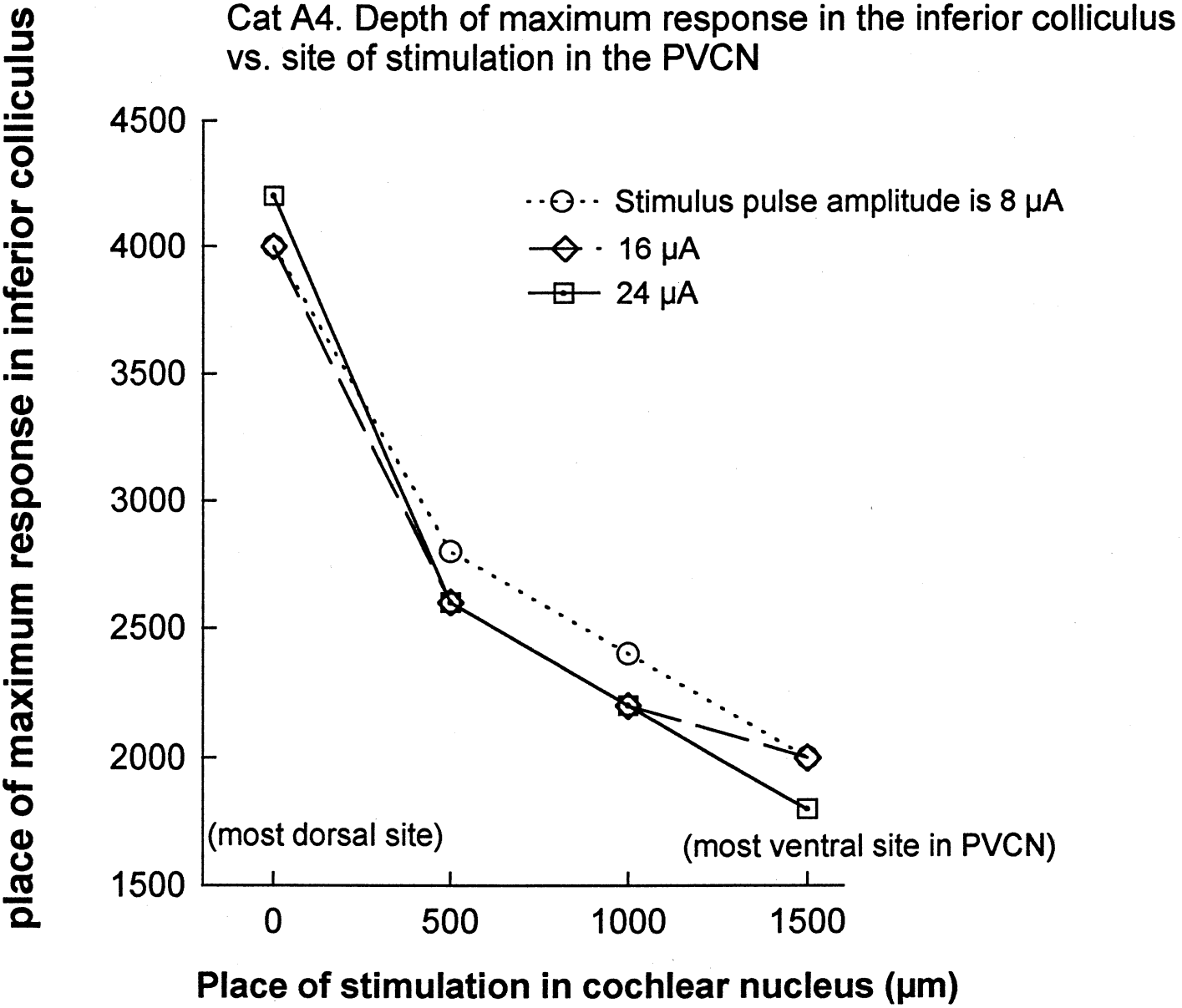
Cat A4. Depth of maximum response in the inferior colliculus vs. site of stimulation in the PVCN
place of maximum response in inferior colliculus
4500
4000
3500
3000
2500
2000
1500
Stimulus pulse amplitude is 8 µA
16 µA
24 µA
(most dorsal site)
(most ventral site in PVCN)
0
500
1000
1500
Place of stimulation in cochlear nucleus (µm)

Figure 5

A

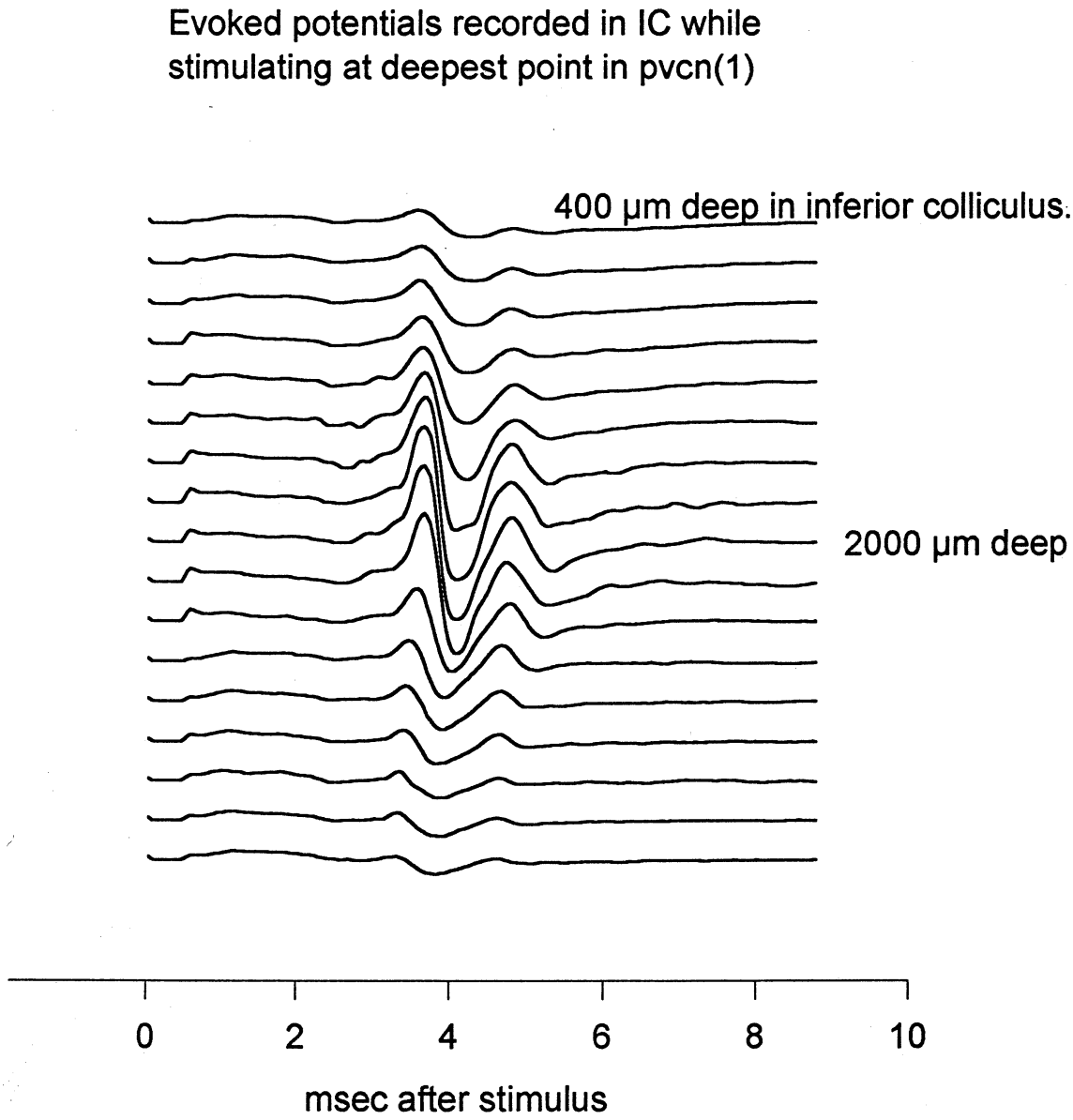
Evoked potentials recorded in IC while stimulating at deepest point in pvcn(1)
400 µm deep in inferior colliculus.
2000 µm deep
0
2
4
6
8
10
msec after stimulus

Figure 6A

B

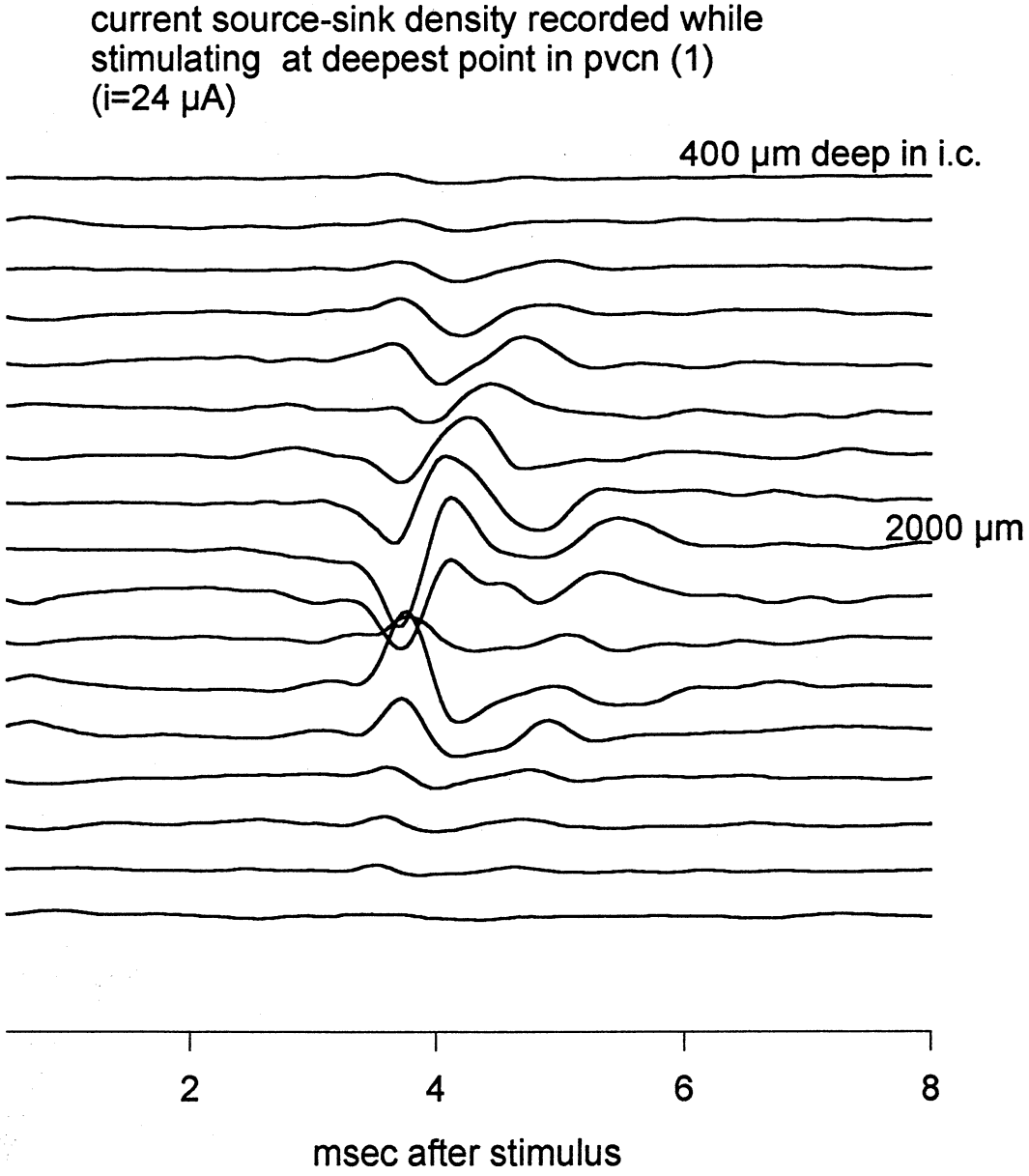
current source-sink density recorded while
stimulating at deepest point in pvcn (1)
(i=24 µA)
400 µm deep in i.c.
2000 µm
2
4
6
8
msec after stimulus

Figure 6B

A

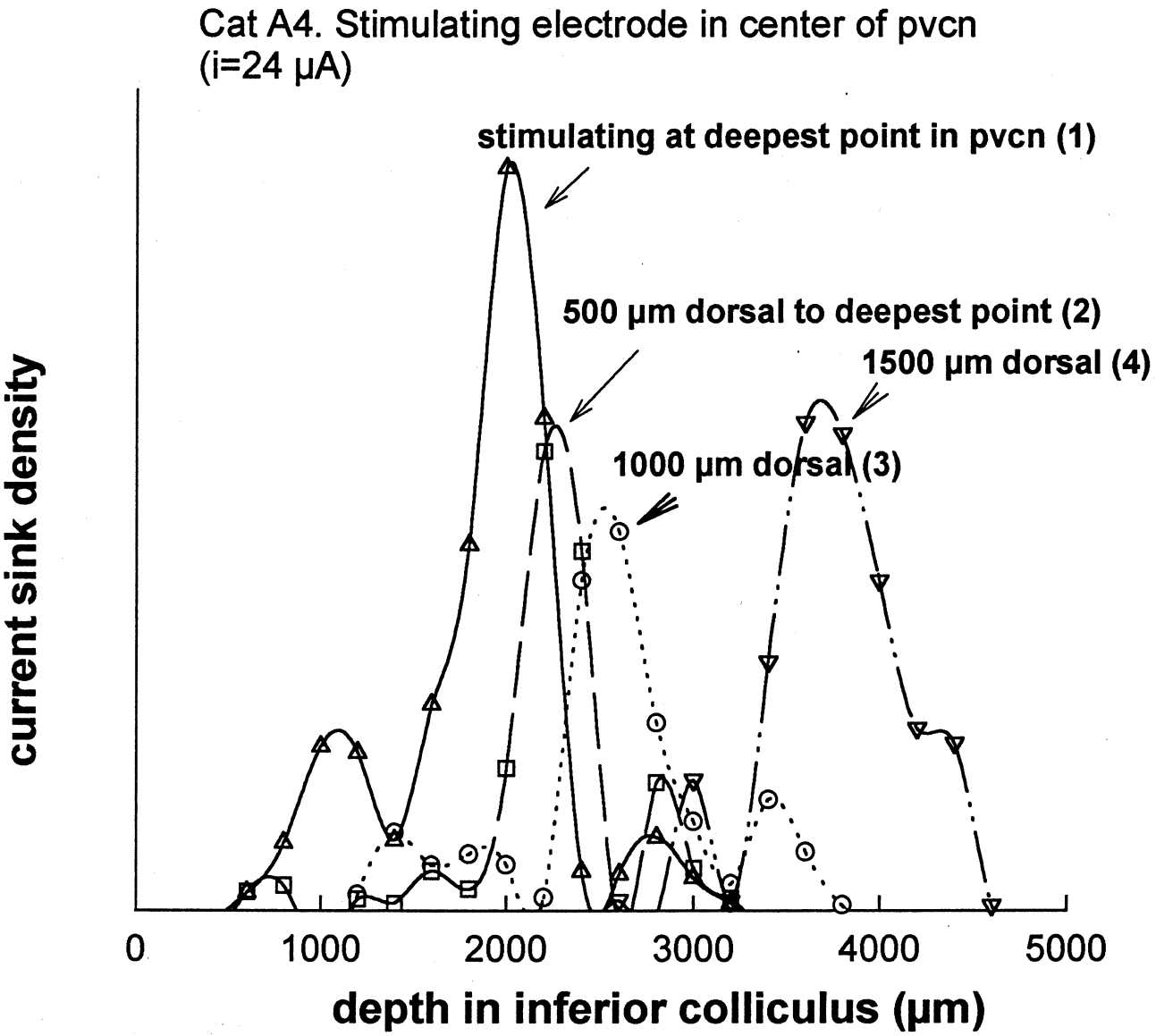
Cat A4. Stimulating electrode in center of pvcn
(i=24 µA)
stimulating at deepest point in pvcn (1)
500 µm dorsal to deepest point (2)
1500 µm dorsal (4)
1000 µm dorsal (3)
current sink density
0
1000
2000
3000
4000
5000
depth in inferior colliculus (µm)

Figure 7A

B

Cat A5. Stimulating electrode near medial border of PVCN (i=20 μA)

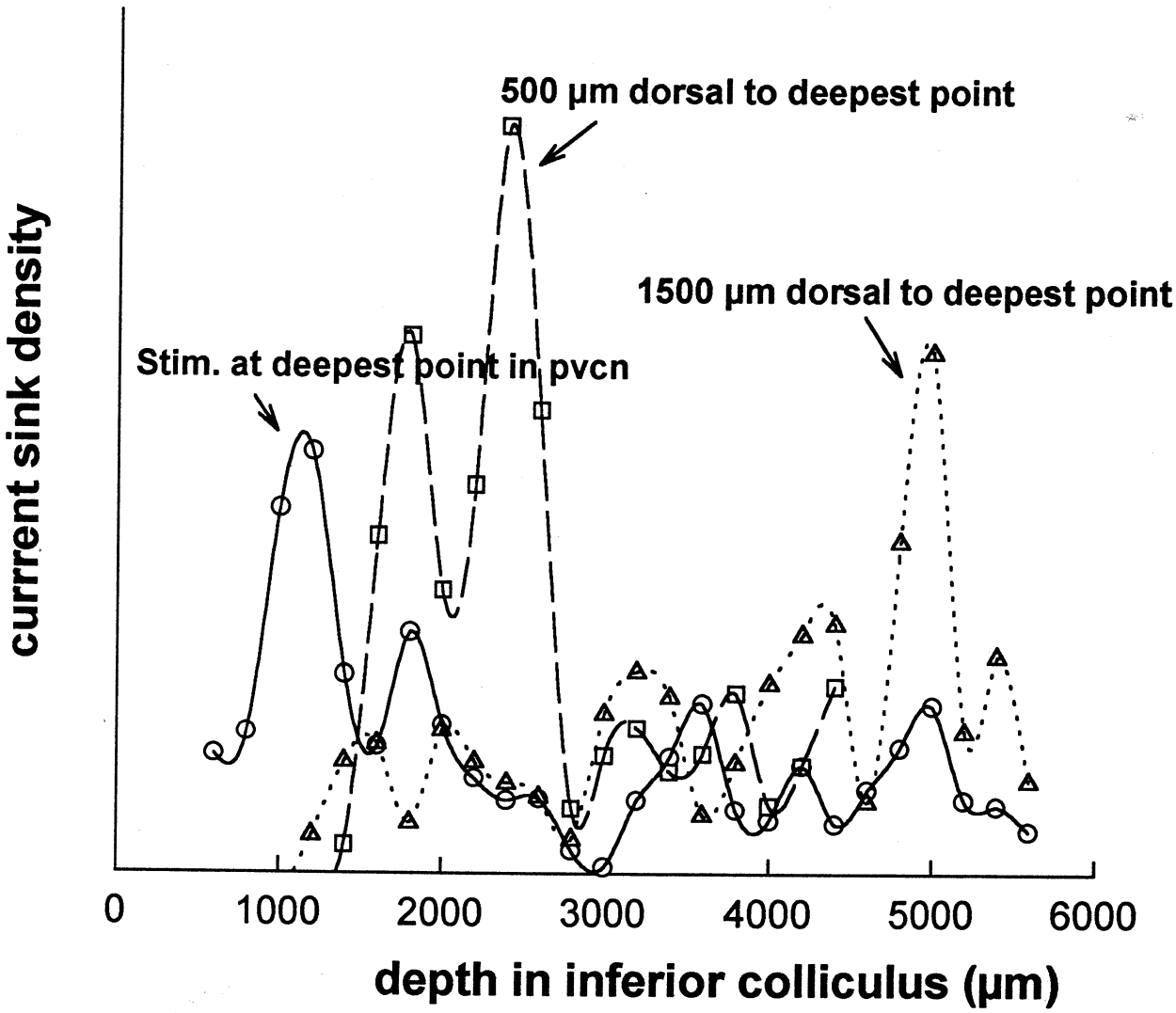

Figure 7B

C

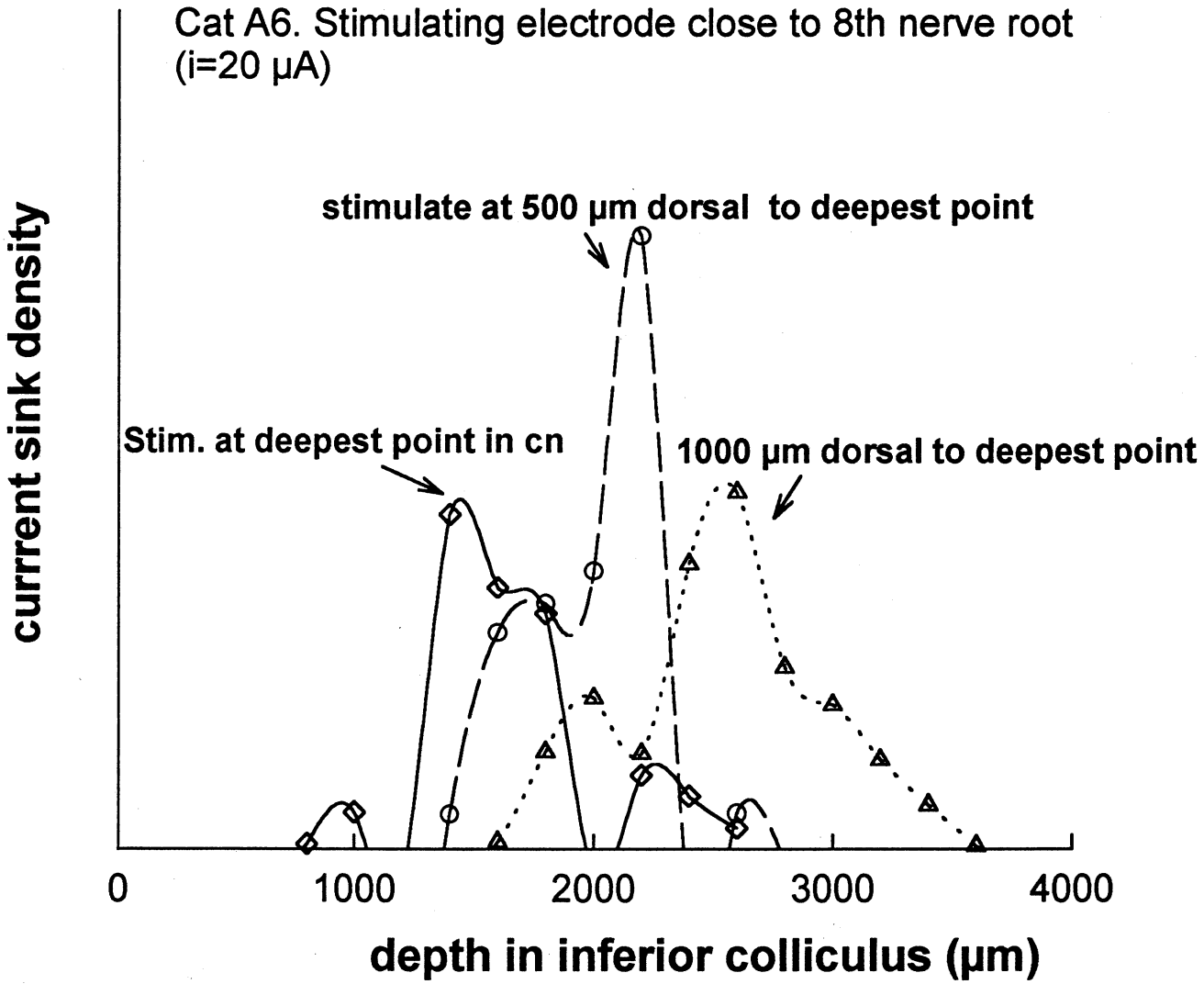
Cat A6. Stimulating electrode close to 8th nerve root
(i=20 µA)
stimulate at 500 µm dorsal to deepest point
Stim. at deepest point in cn
1000 µm dorsal to deepest point
currrent sink density
0
1000
2000
3000
4000
depth in inferior colliculus (µm)

Figure 7C

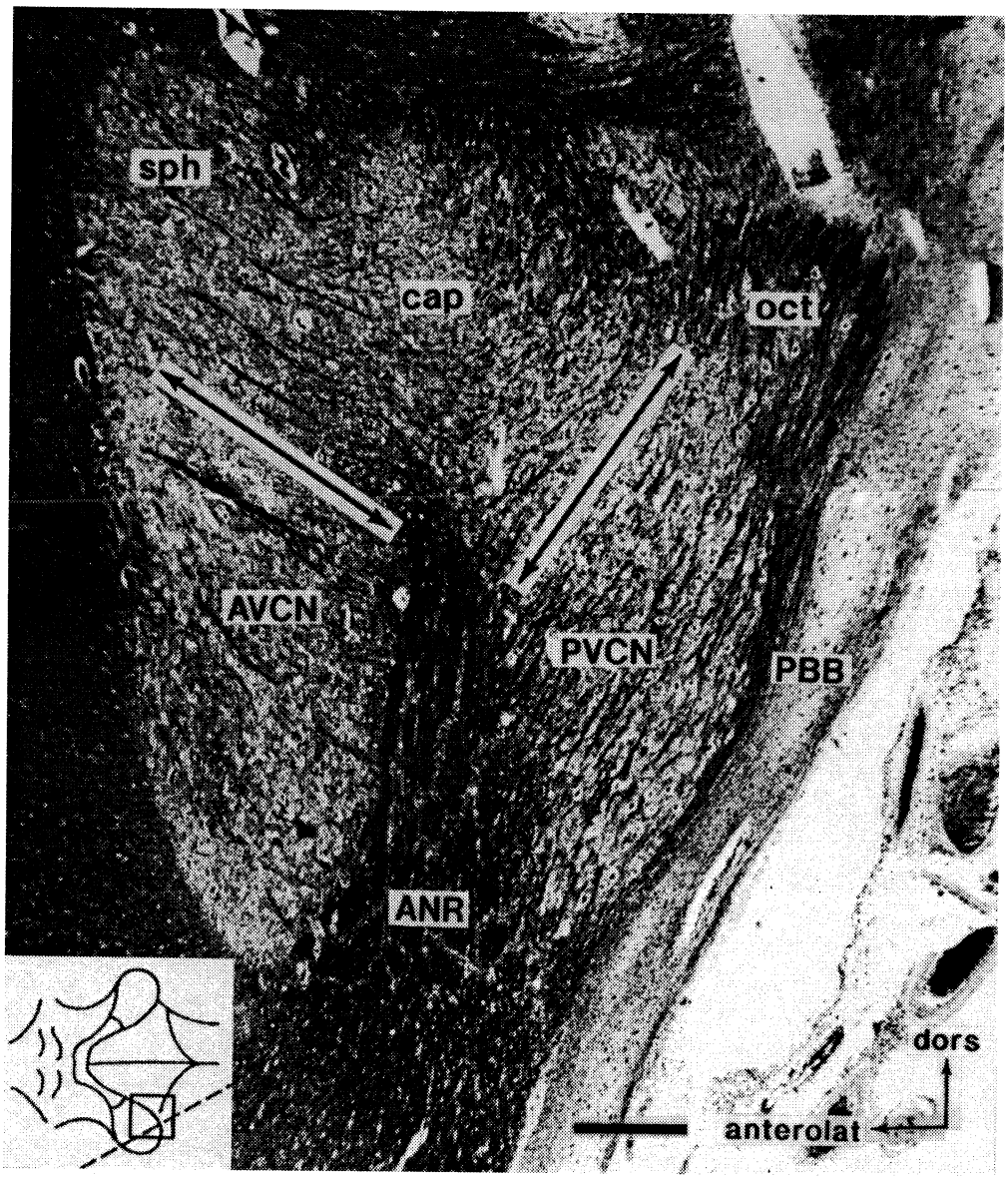

Figure 8

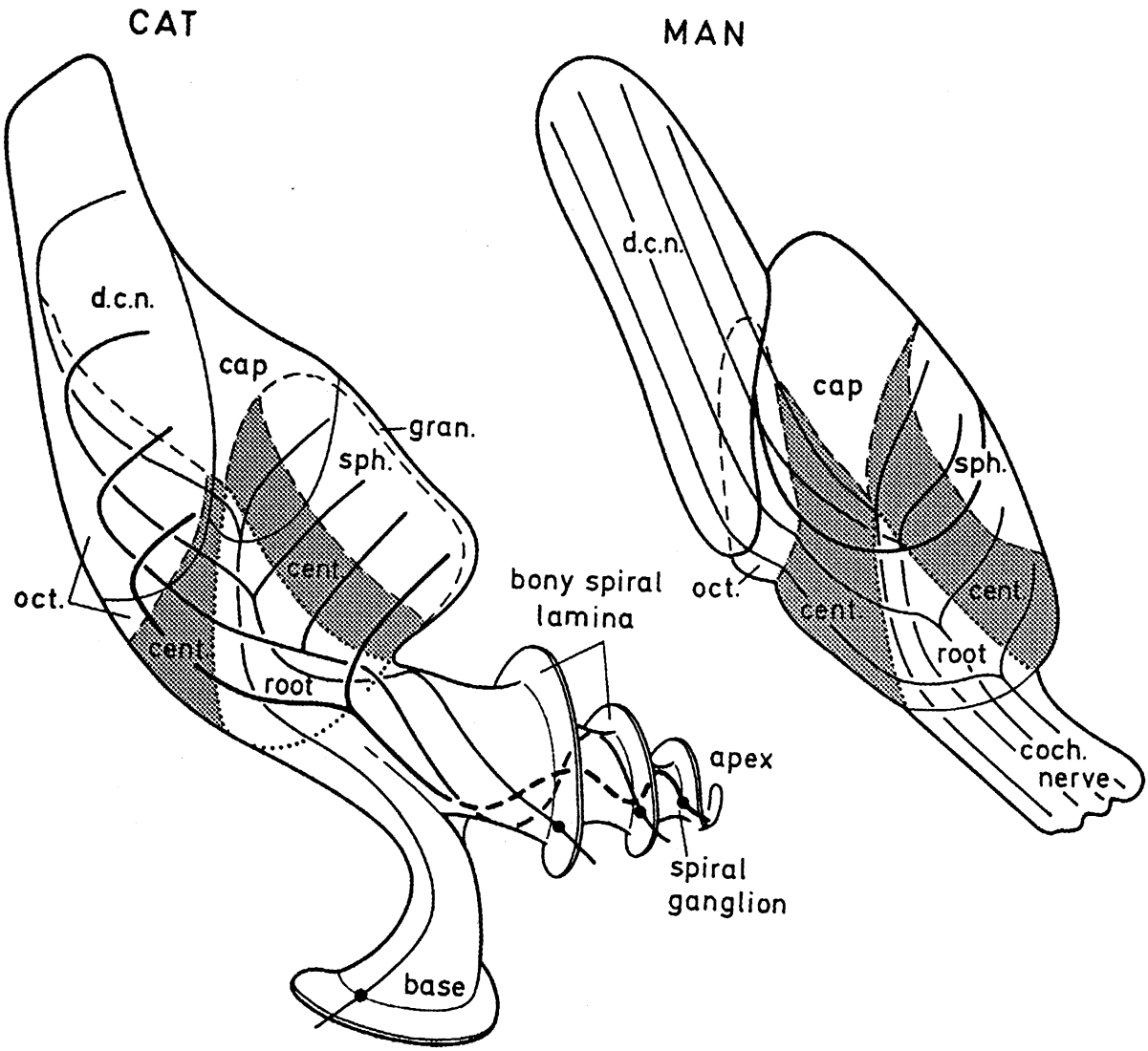
CAT
MAN
d.c.n.
cap
gran.
sph.
cent.
oct.
cent.
root
bony spiral
lamina
apex
spiral
ganglion
base
d.c.n.
cap
sph.
oct.
cent.
cent.
root
coch.
nerve

FIGURE 9